

Hierarchical Terrace Formation in PS-*b*-P4VP(PDP) Supramolecular Thin Films

Wendy van Zoelen, Evgeny Polushkin, and Gerrit ten Brinke*

Laboratory of Polymer Chemistry, Zernike Institute for Advanced Materials, University of Groningen, Nijenborgh 4, 9747 AG Groningen, The Netherlands

Received August 8, 2008; Revised Manuscript Received September 19, 2008

ABSTRACT: The terrace formation behavior of chloroform vapor annealed thin films of asymmetric, low molecular weight comb-shaped supramolecules consisting of a short polystyrene (PS) block and a long supramolecular block of poly(4-vinylpyridine) (P4VP) hydrogen bonded with pentadecylphenol (PDP) on silicon oxide (SiO₂) was examined with atomic force microscopy. During annealing, PS microphase separated from the disordered P4VP(PDP) comb, resulting in the formation of terraces of parallelly oriented microdomains of PS in a matrix of P4VP. Upon evaporation of the solvent, the P4VP(PDP) combs dropped below their order–disorder transition, and formed alternating layers of P4VP and PDP, which for high P4VP(PDP) fractions were also oriented parallel to the substrate. This resulted in terraces of the short P4VP(PDP) length scale within terraces of the PS-P4VP long length scale. Washing away PDP from the thin films with ethanol provided an effective means of studying the morphology of the lowest terrace of the thin films and, for a particular system, also resulted in a uniform monolayer of cylinders with a PS core and a P4VP corona.

Introduction

Due to their well-known ability to microphase separate into ordered structures with a typical length scale of 10 to 100 nm and the obvious connection with nanotechnology applications, block copolymers have been the topic of numerous theoretical and experimental studies,^{1,2} and although the bulk behavior of new types of block copolymers such as rod-coil block copolymers, multiblock copolymers and supramolecular systems still poses new interesting challenges,^{3–5} the bulk phase behavior of “simple” coil-coil diblock copolymers is by now well-understood. At certain temperatures below the order–disorder temperature T_{ODT} , several ordered morphologies such as body centered cubic spheres, hexagonally packed cylinders and lamellae will be formed, depending on the length of the blocks, the Flory–Huggins interaction parameter between the blocks χ and the block composition. Close to the T_{ODT} , other morphologies such as the bicontinuous gyroid or perforated lamellae are also a possibility.⁶ However, the lack of long-range order in the bulk of these structures has very much limited the use of block copolymers in nanotechnology applications. Methods to improve long-range order include the use of large amplitude oscillatory shear, extrusion and electric fields.⁷

At first sight, the use of thin block copolymer films seems to be a simplification, as the ordering now only has to be improved in two dimensions. Namely, for thin enough polymer films the surface interactions are strong enough to align the microphase separated structures either perpendicular or parallel to the surface field. On the other hand, the surfaces on top of and underneath the film also very much complicate the phase behavior. Depending on the film thickness the surface field may vary, resulting in different height-dependent structures.^{8,9} Furthermore, when one of the surfaces is not rigid, such as air, and the surfaces have preferential interactions with one of the blocks, quantization of the film thickness will take place upon annealing, during which the film thickness will adopt a value that is a multiple of the lamellar, cylindrical or spherical period. Nevertheless, thin block copolymer films are promising candidates for nanotechnology applications, and that is why lately a lot of research has been devoted to this topic.^{10–12} But although

some common behavior has been identified, it remains difficult to foretell the thin film behavior of a specific block copolymer system.

The thin film behavior of more exotic block copolymer systems remains even more of a mystery, and especially detailed investigations on supramolecular systems, where block copolymers are complexed with a small molecule through noncovalent interactions, are rare.^{13–16} Supramolecular systems offer the advantage of incorporating new functionalities by altering the small molecule additive and tuning the size of the microphase separated structures without having to synthesize completely new block copolymers. Furthermore, the small molecule can often simply be washed away, resulting in nanoporous structures. Recently van Zoelen et al.¹³ reported on the thin film behavior of high molecular weight PS-*b*-P4VP(PDP) comb copolymers, where pentadecylphenol (PDP) amphiphiles are hydrogen bonded to the poly(4-vinylpyridine) block of a polystyrene-*block*-poly(4-vinylpyridine) (PS-*b*-P4VP) diblock copolymer. In bulk, these systems give rise to microphase separation into so-called structures-*within*-structures, where the P4VP microphase separates from the PDP amphiphiles on a short length scale of ~ 4 nm, and PS and the complete P4VP(PDP) comb microphase separate on a long length scale (10–100 nm) perpendicular to the short length scale.¹⁷ In chloroform vapor annealed thin films, an increased selectivity of chloroform toward the PS block as compared to the pure diblock copolymer was found, resulting in morphology switching of the large length scale for different vapor pressures. At a certain vapor pressure, a bulk lamellar system was on the boundary between the lamellar and cylindrical phase and displayed noncommon terrace formation behavior with the formation of metastable perpendicular lamellae. However, the morphology of the short length scale was not observed, although also not explicitly investigated.¹³ In a recent study on low molecular weight PS-*b*-P4VP(PDP) comb shaped supramolecules, structures-*within*-structures have been observed. At low chloroform vapor pressures and high P4VP(PDP) fractions the large length scale was found to orient perpendicular to the substrate, and the short length scale oriented parallelly.¹⁸ Also in other thin film studies of comb-shaped supramolecules, structures-*within*-structures have only been reported very recently when Albrecht et al.¹⁶

* Corresponding author. E-mail: G.ten.Brinke@rug.nl.

Table 1. Properties of Systems Studied at $T_s = 20\text{ }^\circ\text{C}^a$

sample	f_{P4VP} or f_{comb}	structure			thickness (nm)		
		T0	T1	T2	T0	T1	T2
P3546	0.487	W	W-L	W-L-L	10.8	32.4	54.7
P3546(PDP) _{0.1}	0.551	L	L-L	L-L-L	16.7	35.7	53.9
P3546(PDP) _{0.2}	0.600	C	C-L	C-L-L	16.9	34.0	50.7
P3546(PDP) _{0.5}	0.699	C	C-C	C-C-C	19	38	54
P3546(PDP) _{1.0}	0.787	S	S-C	S-C-C	17	34	55
P110	0.305						
P110(PDP) _{0.1}	0.362	L	L-L	L-L-L	22.4	44.4	66.3
P110(PDP) _{0.2}	0.409	L	L-L	L-L-L	20.4	41.9	60.9
P110(PDP) _{0.5}	0.518	L	L-L	L-L-L	19.2	41.9	67.4
P110(PDP) _{1.0}	0.631	C	C-C	C-C-C	20	44	68
P110(PDP) _{1.5}	0.701	C	C-C	C-C-C	20	47	73
P141(PDP) _{1.0}	0.428	L	L-L	L-L-L	15.7	34.6	55.0

^a Subscripts (0.1, 0.2, etc.) denote the number of PDP molecules per pyridine ring. W = half-lamellar wetting layer, L = lamellar, C = PS cylinders in P4VP(PDP) matrix, and S = PS spheres in P4VP(PDP) matrix, PL = perforated PS lamellae. All structures are parallel to the surface; except for the transition morphologies, no perpendicular structures have been observed. The thickness of the lamellar structures can be determined relatively accurately, the thickness of other terraces should only be regarded as an indication. P110 did not form any terraces or microphase separated structures under the used conditions.

reported on the thin film morphologies of poly(2-vinylpyridine)-*block*-poly(ethylene oxide) (P2VP-*b*-PEO) diblock copolymers, complexed with wedge-shaped amphiphilic sulfonic acid molecules able to form liquid-crystalline structures. They found that the short length scale preferentially oriented parallel to both the substrate and the air interface, resulting in perpendicularly oriented PEO microdomains and terraces that had a step height of one smectic layer.¹⁶

In the present study, we report on the hierarchical structure formation of chloroform vapor annealed PS-*b*-P4VP(PDP) comb copolymer thin films on silicon oxide. In contrast to our previous publication, which considered asymmetric systems with a large PS block and high molecular weights, the present study focuses on systems that are asymmetric with a large comb fraction and have a significantly lower molecular weight. As will be explained, chloroform vapor annealing of these systems at higher vapor pressures than used by Tung et al.¹⁸ results in hierarchical terrace formation of terraces with a large length scale step height that are subdivided into terraces with the step height of the short length scale. As opposed to the bulk systems, the long and the short length scale are oriented parallel instead of perpendicular to each other.

Experimental Section

Materials. Three PS-*b*-P4VP diblock copolymers were acquired from Polymer Source Inc. and used as received: P3546 ($M_n(\text{PS}) = 20000\text{ g/mol}$, $M_n(\text{P4VP}) = 19000\text{ g/mol}$ and $M_w/M_n = 1.09$), P110 ($M_n(\text{PS}) = 47600\text{ g/mol}$, $M_n(\text{P4VP}) = 20900\text{ g/mol}$ and $M_w/M_n = 1.14$) and P141 ($M_n(\text{PS}) = 42100\text{ g/mol}$, $M_n(\text{P4VP}) = 8100\text{ g/mol}$ and $M_w/M_n = 1.08$). Homopolymer P4VP with a molecular weight of 50000 g/mol was obtained from Polysciences, Inc. and used as received. 3-*n*-Pentadecylphenol was purchased from Aldrich and was recrystallized twice from petroleum ether (40–60 w/w) and dried in a vacuum at 40 °C.

Film Preparation. Silicon substrates of $\sim 1\text{ cm}^2$ with a native silicon oxide layer (SiO_2) on the surface were cleaned by CO_2 snow jet cleaning and used immediately afterward. PS-*b*-P4VP (or P4VP) and PDP (in different stoichiometrical amounts, see Table 1 for details) were dissolved in chloroform and shaken for at least two hours to yield 1–2 wt % stock solutions. These solutions were diluted and spin coated onto the freshly cleaned silicon wafers at speeds between 2000 and 5000 rpm to give films of the desired thickness (~ 70 – 80 nm as judged from AFM scratch tests and the dark brown color of the films).¹³ After spin coating, a scratch was

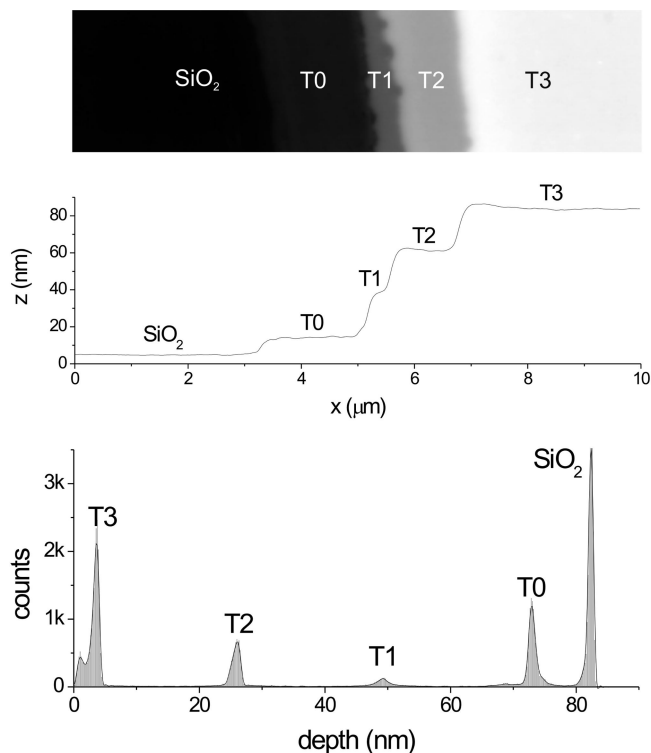


Figure 1. (Top) AFM height image and (middle) profile of P3546 annealed at $T_s = 20\text{ }^\circ\text{C}$ for 21 h. (Bottom) Depth profile (gray droplines) and FFT smoothing (black line). The shoulder next to the T3 peak is caused by the slight bump at the onset of the terrace.

made in the polymer film with a razor blade, being careful not to damage the silicon itself.

Chloroform vapor annealing was carried out in a small sealed chamber. The temperature of the polymer samples on silicon T_p was kept at 24 °C with the use of a Tamson TC heating circulator, while a small solvent reservoir of which the temperature T_s was adjusted between 19 and 21 °C using a Lauda RC6 CP refrigerated circulator was included. The temperatures of the sample and the solvent reservoir were kept constant to within $\pm 0.05\text{ }^\circ\text{C}$, while T_s was always lower than the ambient temperature to avoid condensation on the chamber walls. By variation of the solvent temperature, the solvent vapor pressure inside the chamber could be adjusted, resulting in different swelling ratios of the polymer films.¹⁹ After annealing the lid of the chamber was lifted, and solvent in the films evaporated within a fraction of a second. Unless stated otherwise, samples have been annealed for a period of 20–24 h. For clarification of the terrace structures, PDP was gently washed from the films by immersion in ethanol for approximately 30 s, after which the films were blown dry in a stream of nitrogen. In order to reveal the structure of the bottom terrace, the films were treated in ethanol with ultrasound for $\sim 3\text{ min}$, resulting in removal of the top layers.

Characterization. Atomic force microscopy (AFM) measurements were carried out on a Digital Instruments EnviroScope AFM equipped with a Nanoscope IIIa controller in tapping mode using Veeco RTESPW silicon cantilevers ($f_0 = 240$ – 296 kHz and $k = 20$ – 80 N/m as specified by the manufacturer). AFM images were typically obtained with a frequency of 1 Hz/line and always included a part of the bare silicon surface on the left. For measurement of the terrace heights, a plane was fitted to the bare substrate of a scan with an aspect ratio of 1:8 to minimize distortion along the slow scanning axis, after which the height was analyzed using a depth profile (see Figure 1). For publication, most pictures (except Figure 1) have been treated with a flattening filter in order to facilitate the perception of the terrace microdomain structures, rather than focusing on the height difference between the terraces.

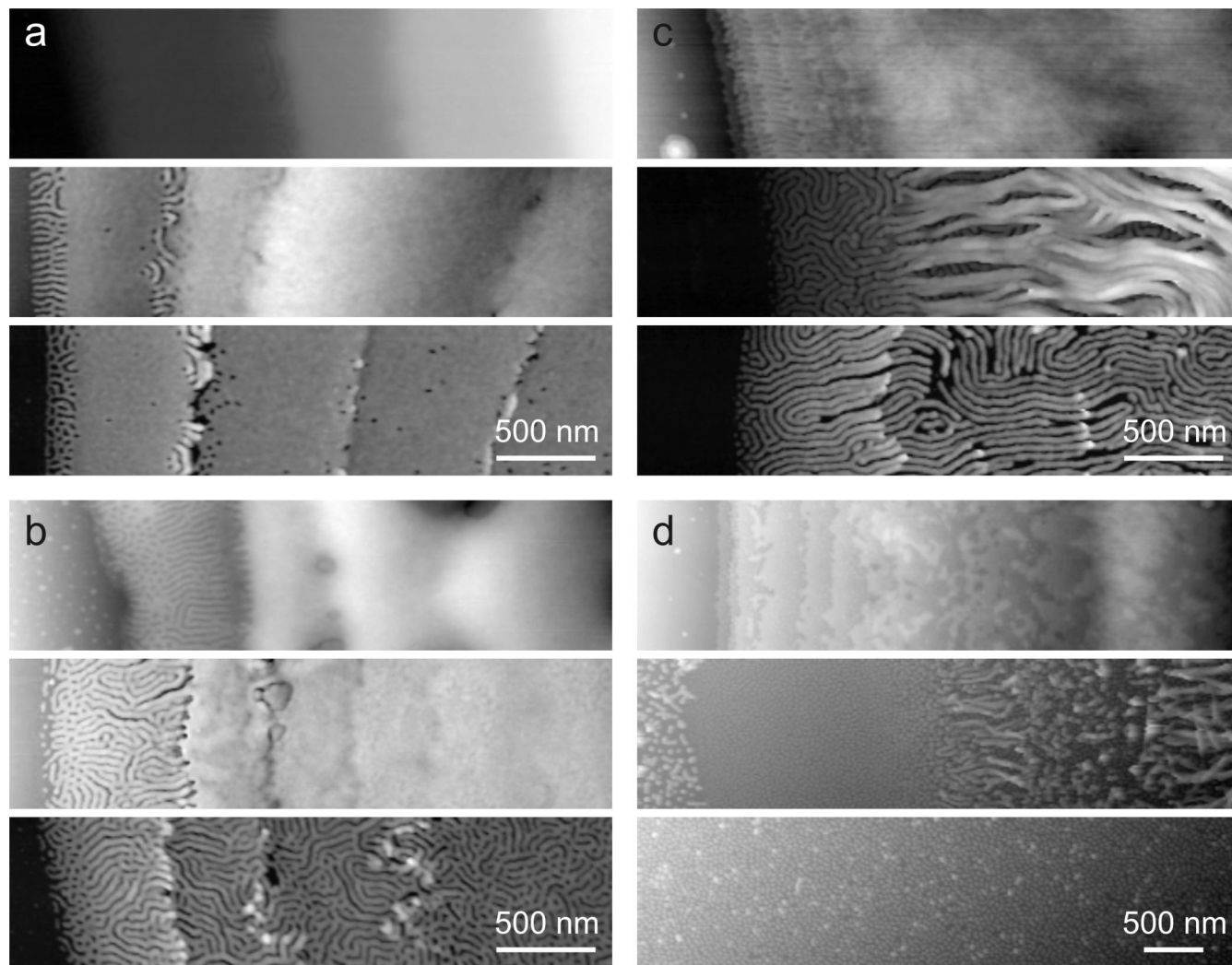


Figure 2. AFM height images of annealed thin films before rinsing with ethanol (upper), after gentle rinsing with ethanol (middle), and after ultrasound treatment (lower) of (a) P3546(PDP)_{0.1}, (b) P3546(PDP)_{0.2}, (c) P3546(PDP)_{0.5}, and (d) P3546(PDP)_{1.0}. Δz ranges from 25 to 150 nm, however, either plane fit or flattening filters have been used on the images to gain an optimal contrast for viewing the microdomain structures. After gentle rinsing of P3546(PDP)_{1.0} (d), the scratch on the left side has filled with small rods and spheres that have been washed off from the film. After ultrasound treatment, the whole film therefore had approximately the same height and the scratch could not be located anymore with an optical microscope, hence the picture after ultrasound is one of the bottom of the bulk of the film.

Results and Discussion

First, a ~ 75 nm scratched film of the bulk lamellar diblock copolymer P3546 was swollen using a T_s of 20 °C, resulting in swelling of the film to approximately 2 – 2.5 times the original film thickness, as judged from the color change from a dark brown to a light blue film. During annealing, the scratch is refilled with polymer, resulting in terrace formation at the edge of the scratch. Figure 1 shows the resulting AFM image after fitting a plane to the bare substrate of a film that was annealed for 21 h, clearly revealing the different terrace heights also shown in the cross-section. The depth analysis of the film is also shown, where the peaks correspond to the depths of the different terraces measured from the highest point in the film. A wide terrace (T0, T2, and T3) corresponds to a large peak area, whereas a shorter terrace (T1) results in a smaller peak. The sharpness of the peak is a measure for the thickness variations within the terrace. The terrace heights can be determined from the peak positions and have been summarized in Table 1. The height of T0 (10.8 nm) is half the value of the thickness increases for the other terraces (~ 22.0 nm on average), showing that a half-lamellar wetting layer is formed at the silicon interface, an effect that is well-known for thin films of PS-*b*-P4VP diblock copolymers. Due to the strong interaction of P4VP

with the SiO₂ interface, and the lower surface free energy of PS, PS-*b*-P4VP diblock copolymers exhibit asymmetric wetting conditions, resulting in terrace heights of $(n + 1/2) L$.²⁰

In our previous study on PS-*b*-P4VP(PDP) comb-copolymer thin films, we found that PS-*b*-P4VP(PDP) supramolecules with at least one PDP molecule per pyridine ring exhibited symmetric wetting conditions, due to the favorable interactions of PDP with the air interface as opposed to the pure diblock where PS preferentially segregates at the air interface. One could wonder if the addition of only a very small amount of PDP could result in a neutral air interface. The AFM height image of a P3546(PDP)_{0.1} thin film (Figure 2a) shows that as little as 10% of PDP molecules per pyridine ring is already enough to alter the wetting conditions. Again a scratch has been made in the film before annealing, this time resulting in dewetting of the film away from the scratch edges, indicating that the interaction of the P4VP(PDP) comb with the SiO₂ substrate is less favorable than the interaction of pure P4VP with SiO₂. The different terraces can again be observed, although the terrace widths are on average smaller than for the pure diblock copolymer, most likely due to the dewetting mechanism, compressing instead of stretching the material at the scratch edges. The exact width of a terrace is the result of the interplay between the initial film

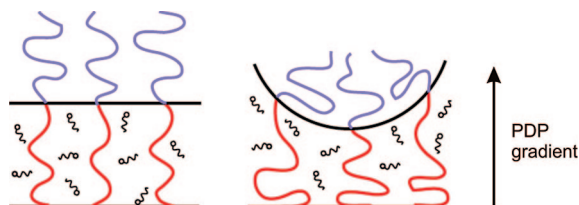


Figure 3. Schematic picture of the influence of the PDP gradient. On the left side the situation of a surface that is equally attractive toward P4VP and PDP is sketched. On the right side, the PDP gradient increases the spacing between the P4VP chains near the PS-P4VP interface, inducing curvature.

thickness, the angle of the scratching knife, the mobility and the surface interactions, and can not be used as an absolute measure. The terrace heights were again obtained from a depth profile and are summarized in Table 1. The height of T0 (16.7 nm) is now almost identical to the thickness increase of the other terraces (~ 18.6 nm), indicating symmetric wetting conditions. As observed in bulk systems, the overall thickness of the lamellae has been reduced compared to the pure diblock copolymer as a result of the presence of PDP.²¹ Gentle washing of the film in ethanol to remove PDP more clearly reveals that the surface layers of the terraces have remained lamellar (middle picture of Figure 2a). Due to the relatively high P4VP(PDP) fraction in the used systems, ultrasound treatment of the films in ethanol results in exfoliation of the top layers of terraces, whereas the bottom terrace remains fixed to the substrate due to the strong interactions of P4VP with SiO₂. This is an easy method to reveal the structure of the bottom terrace, which, in the case of P3546(PDP)_{0.1} is also lamellar with some dot defects. The transitions to T0 and T1 contain perpendicular lamellae and perforated lamellae. For theoretical papers that explain transition morphologies, see refs 8 and 9.

Addition of somewhat more PDP results in a more striking difference. As known from our previous study, chloroform is a selective solvent toward PS in the case of PS-*b*-P4VP(PDP) comb-shaped supramolecules while it is a nonselective solvent for the pure diblock copolymer. The reason for this is not clear, although arguably, the exact selectivity is a function of the P4VP(PDP) comb fraction and the stoichiometric amount of PDP in that comb. Nevertheless, taking into account that bulk P3546 has a lamellar structure, whereas P3646(PDP)_{1.0} forms PS cylinders in a matrix of P4VP(PDP), we can assume that at a certain composition while swelling at a T_s of 20 °C, P3546(PDP)_x is on a phase boundary between lamellae and cylinders for a certain x value. This is most likely the case for P3546(PDP)_{0.2}. T0 exhibits a stripe/dot pattern, whereas the higher terraces remain lamellar. After washing and ultrasound treatment (Figure 2b), the careful conclusion can be drawn, that only the bottom layer shows this stripe/dot pattern, whereas the layers on top remain lamellar.

Now that the top and bottom layers exhibit different morphologies, one could argue that the boundary conditions are in fact not symmetric, and to quite a large extent this is also true. Until now, we treated both interfaces as being selective toward the entire P4VP(PDP) comb, but of course this is an oversimplification of the matter. The alkyl tails of PDP have a very low surface free energy, while on the other hand we have shown that the interaction of SiO₂ with P4VP is strong enough to withstand ultrasound treatment in ethanol, a good solvent for P4VP. This means, that air is selective toward PDP, while SiO₂ is P4VP selective. The consequence is that there will be a PDP concentration gradient away from the SiO₂ interface. The slightly higher concentration of PDP several nanometers away from the SiO₂ surface is just enough to change the morphology to a mixture of perforated lamellae and cylinders (Figure 3). The

preferential interaction of PDP with air does not have a striking influence on the morphology, and the effect also does not exceed the first layer, explaining why only the bottom layer exhibits a different morphology.

For an even higher amount of PDP as in P3546(PDP)_{0.5} one would now expect an all cylindrical morphology and that this is the case can be seen in Figure 2c. However, another feature can also be detected. After a close look at the boundary region between the polymer film and the SiO₂ interface, smaller terraces can be observed, while there also is a presence of the large length scale terraces forming the PS cylinders, which can clearly be seen after washing of the sample. So to speak, the large terraces are subdivided into several smaller terraces. This effect is even more pronounced for P3546(PDP)_{1.0} as can be seen in Figure 2d. The structure of the bottom layer in this case consists of a mixture of spheres and short cylinders, again caused by the PDP concentration gradient. The higher terraces consist of parallel cylinders, with transitional perpendicular cylinders in between all terraces. The depth profile also clearly shows the hierarchical terrace structure. A magnification of the lowest terraces and the depth profile are given in Figure 4.

For the two samples with the lowest amounts of PDP, we have not taken into account nor observed the small length scale structure of the P4VP(PDP) comb. This is not surprising, as we have used ratios of 0.1 and 0.2 PDP units per pyridine ring. From previous studies on P4VP(PDP) supramolecules, it is known that the T_{ODT} of P4VP(PDP) drops from ~ 62 °C for a 1:1 ratio of PDP:P4VP to ~ 47 °C for a 0.5:1 ratio and even lower values for smaller amounts of PDP.²¹ Since we additionally swell our systems to ~ 2.25 times the original film thickness, further shielding the interactions between P4VP and PDP, we have been far above the order–disorder transition of the P4VP(PDP) comb during swelling, and presumably only very close to the ODT after solvent evaporation, explaining why the small length scale structure was not observed.

To corroborate these assumptions, we have swollen P4VP(PDP)_x thin films with $x = 0.2, 0.5$ and 1.0 under the same conditions ($T_s = 20$ °C) for 2 h. Longer annealing times only resulted in more dewetting of the films due to the high mobility of the systems, but did not have any effect on the ordering in the films, indicating that the films are indeed disordered during annealing. Films of P4VP(PDP)_{1.0} seriously dewetted, however, the results of swelling P4VP(PDP)_{0.2} and P4VP(PDP)_{0.5} can be found in Figure 5. For P4VP(PDP)_{0.2} indeed no terrace formation can be observed, except for a very small step at the onset of the P4VP(PDP) layer, which may indicate that the system is near its ODT after evaporation of the solvent. P4VP(PDP)_{0.5} clearly shows the formation of terraces for lower parts of the film. Higher areas do not display distinct terrace formation due to the decreased alignment effect in the middle of the film. The depth profile shows that the alignment effect continues for a film thickness of up to 45 nm. This value is dependent on the ratio of P4VP:PDP, and will be higher for more equal amounts of pyridine rings and PDP. Recall that the alignment of the P4VP(PDP) layers spanned the entire 60 nm film thickness shown of P3546(PDP)_{1.0} (Figure 3d and Figure 4), while only the first few layers of P3546(PDP)_{0.5} were aligned.

In bulk PS-*b*-P4VP(PDP) systems, the short length scale is always oriented perpendicular to the large length scale, while the terrace structures of P3546(PDP)_{0.5} and P3546(PDP)_{1.0} indicate that both the large and small length scale are oriented parallel to the surface. This seems to be in contradiction, but can easily be explained. During swelling, the P4VP(PDP) comb is above its order–disorder transition and terraces of parallel oriented PS cylinders in a matrix of P4VP(PDP) are formed, however, during solvent evaporation, the P4VP(PDP) comb drops below its order–disorder transition and forms layers which

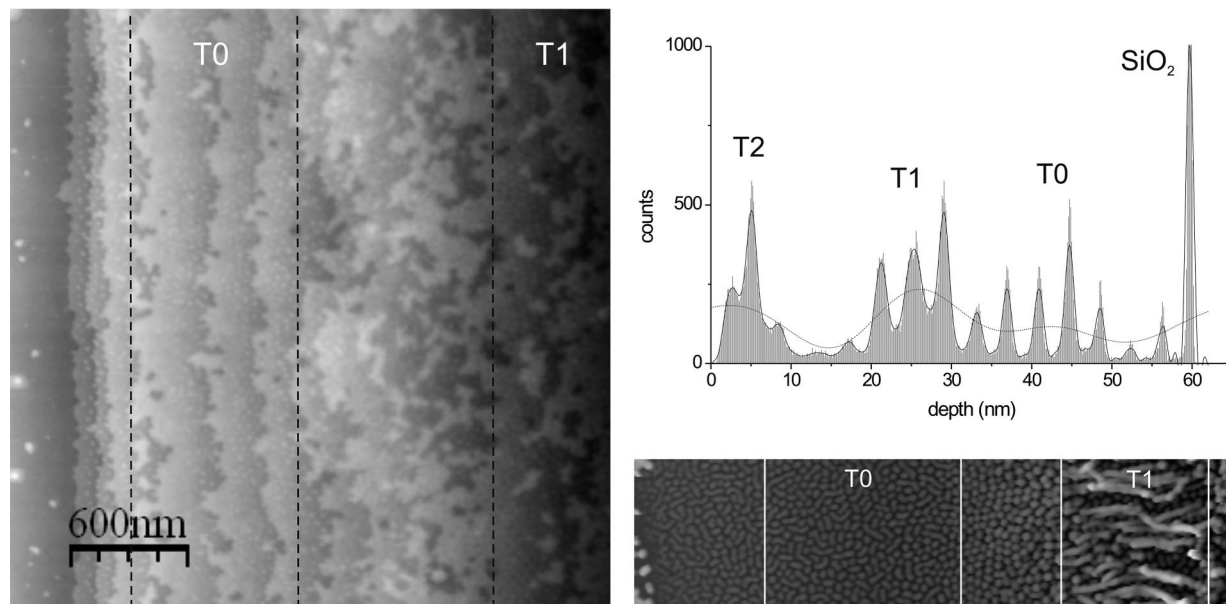


Figure 4. AFM height image ($\Delta z = 25$ nm, data has been flattened) and depth profile of P3546(PDP)_{1.0}. The black line is an FFT smoothing of the data, the distance between the small peaks is ~ 4 nm. The dotted line is the result of more drastic data smoothing, from which can be concluded that the smaller terraces are a part of 3 large length scale terraces. The right bottom picture ($\Delta z = 70$ nm) shows the structure of T0 and the transitional layer of perpendicular cylinders as well as small parts of the bottom layer and the top layer of parallel cylinders of T1 after washing.

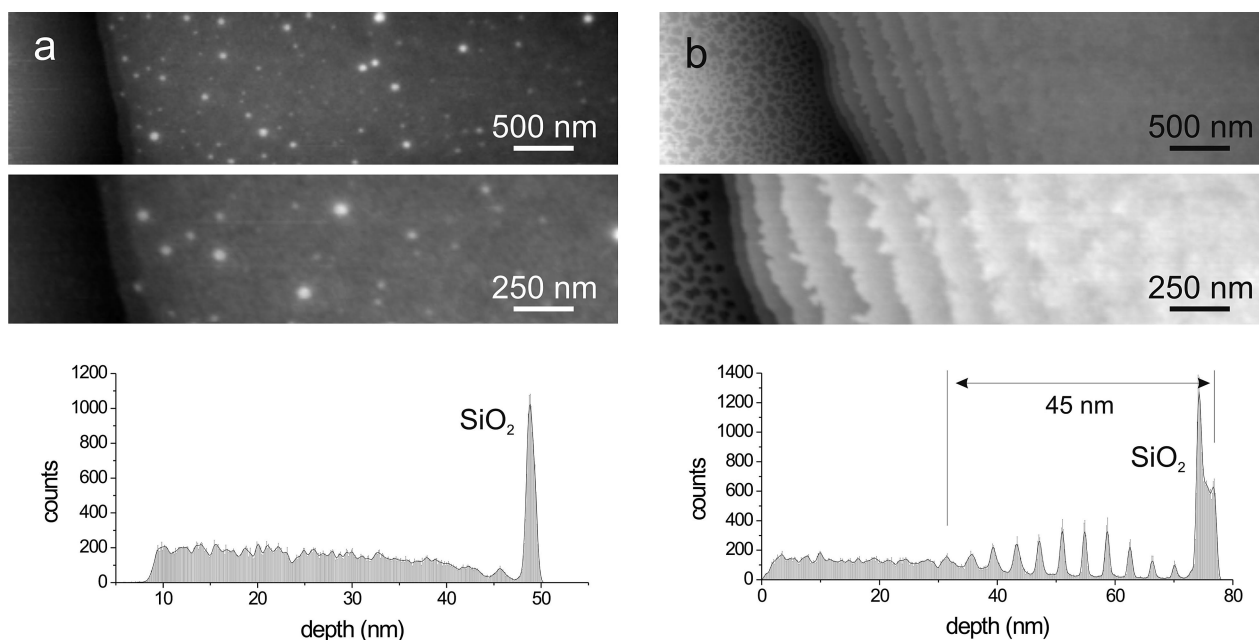


Figure 5. Height AFM and depth profiles of (a) P4VP(PDP)_{0.2} and (b) P4VP(PDP)_{0.5} after 2 h of annealing at $T_s = 20$ °C. The bright dots in a) are likely caused by crystallization of PDP. The scratch in part b) is covered with a perforated layer of PDP or P4VP(PDP); hence, the shoulder of the high peak (near 80 nm) in the depth profile corresponds to the SiO₂ surface.

spontaneously orient parallel to the surface due to the preferential interaction of P4VP with SiO₂ and of PDP with air. In the ideal case, the PS cylinders would now orient perpendicular to the surface, nevertheless, as the solvent evaporates too fast for the large structures to reorient, what remains is a hybrid structure where both the large length scale as well as the small length scale are oriented parallel to the surface (Figure 6). The alignment effect is the strongest near the straight SiO₂ interface and will presumably be somewhat less pronounced near the less rigid air interface. In the middle of thicker terraces, the alignment effect of the surfaces is diminished and the alignment will probably not be strictly parallel.

We have also annealed P110 systems in a similar fashion, giving comparable results as the P3546(PDP)_x systems, however, due to its higher molecular weight and hence lower mobility as compared to P3546, swelling P110 at $T_s = 20$ °C does not result in terrace formation nor in microdomain structure formation. Addition of even a small amount of PDP imparts considerable mobility and results in a lamellar morphology for P110(PDP)_x with $x = 0.1, 0.2$, and 0.5 , resulting in comparable structures as for P3546(PDP)_{0.1} when swelling at $T_s = 20$ °C. A higher amount of PDP is necessary to induce a phase transition to PS cylinders, and that has occurred for P110(PDP)_{1.0}, which exhibits an all cylindrical morphology comparable to P3546(PDP)_{0.5}, but

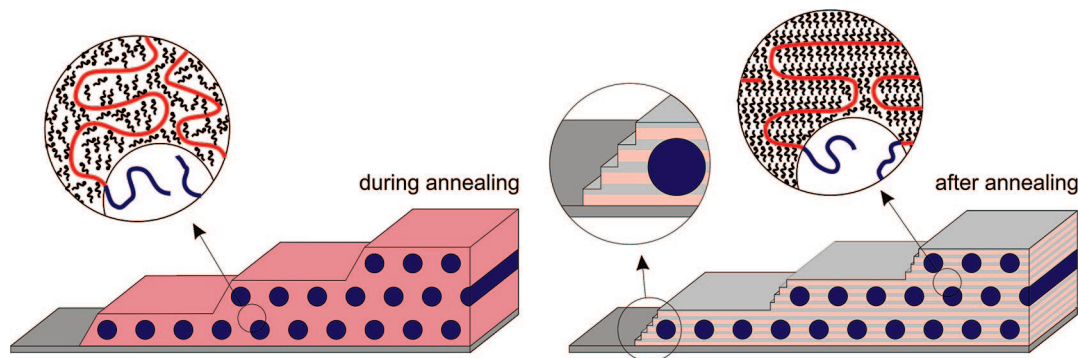


Figure 6. Schematic drawing of terrace formation. During annealing P4VP(PDP) is disordered and PDP merely acts as a selective solvent for P4VP, while the PS-*b*-P4VP block copolymer forms terraces of parallel oriented cylinders. During solvent evaporation P4VP(PDP) drops below its ODT and forms terraces which are also parallel to the surface.

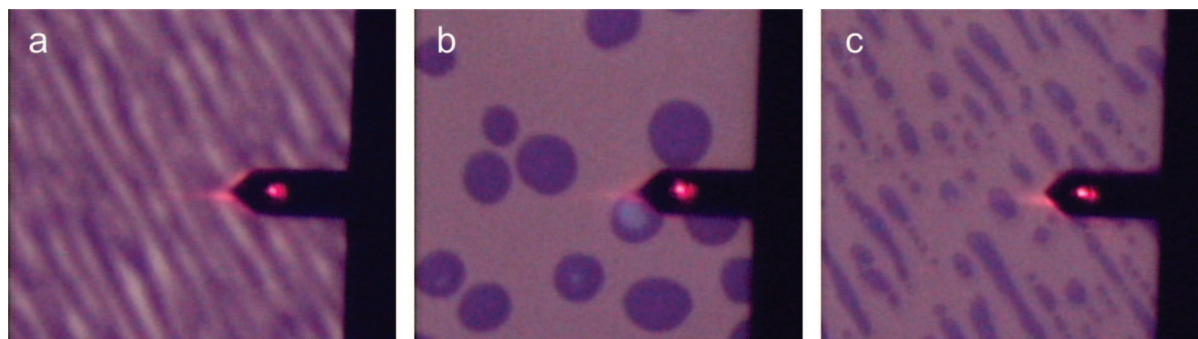


Figure 7. Optical microscopy pictures of ~ 75 nm thin films annealed at $T_s = 20$ °C for 21 h. (a) P110; (b) P110(PDP) $_{0.2}$, and (c) P110(PDP) $_{1.0}$. In parts b and c, (dark) islands of T3 on surroundings of T2 can be observed. The length of the cantilever is ~ 125 μm .

just as for this system, the terrace-*within*-terrace structure is not as clear as for P3546(PDP) $_{1.0}$ and can only be observed in a few layers close to the SiO $_2$ interface. In this case, this is likely caused due to the lower P4VP fraction, complicating the movement of the P4VP chains in an orientation parallel to the PS cylinders.

Furthermore, at this higher fraction of PDP, the overall mobility of the sample has decreased somewhat, which is illustrated in Figure 7. Figure 7a shows the surface structure of the pure diblock copolymer P110 after annealing as observed with an optical microscope. The surface appears almost exactly the same as it did before annealing, with striations originating from the center of the film caused by the volatile evaporation of chloroform, illustrating that there has hardly been any motion in the sample. P110(PDP) $_{0.2}$ on the other hand is very mobile and has formed circular terraces (Figure 7b). P110(PDP) $_{1.0}$ has also formed terraces (Figure 7c), however, the shape of the striations can still be observed in the terraces, indicating that chain movement is slower as compared to samples with a lower amount of PDP. To summarize, addition of PDP induces mobility to PS-*b*-P4VP, however, systems with lower amounts of PDP are more mobile than systems with higher amounts of PDP. The reason for this is not at all clear, but should be connected to the relative solubility of PDP in PS and P4VP. In bulk comb-copolymer systems, a small amount of PDP is known to be soluble in PS, acting as a plasticizer.²² The solubility of PDP in PS may be dependent on its own concentration and might also be influenced by CHCl $_3$, in its turn influencing the mobility. An obvious difference in the swelling ratio of the different films during annealing was never observed, although slight changes can not be excluded.

Addition of an even higher amount of PDP also results in terraces, which have a cylindrical morphology. Figure 8a shows the height AFM image after ultrasound treatment of P110(PDP) $_{1.5}$, where the bottom layers of the transition from

T0 to T1 and T1 to T2 have been depicted. There it can be seen that the thickness of the cylinders at the first transition increases rather much, but at the second transition, this effect is negligible. This means that if a film with a minimum thickness of T1 (47 nm) is cast, a monolayer of cylinders with uniform thickness can simply be obtained after annealing and subsequent ultrasound treatment of the film. However, the cylinders are not aligned very well and the monolayer also contains a large amount of classical defects and defects in the form of interconnections between cylinders.²³ The first problem can be solved by annealing the film at a higher T_s of 21 °C, increasing the mobility of the chains and thereby the alignment of the cylinders. However, due to the selectivity of chloroform toward PS, the system is now also closer to a (perforated) lamellar morphology and contains a substantial amount of interconnection defects even though the overall alignment is better (Figure 8b). Less defects appear if a film is annealed at a T_s of 19 °C and hence closer to a strictly cylindrical morphology, however, then the alignment is somewhat worse because of the lower mobility (Figure 8c). Combining the two methods, whereby the films are first annealed at $T_s = 21$ °C for alignment, and subsequently at 19 °C for defect removal provides the answer. Figure 8d shows a monolayer of ordered cylinders with a PS core and a P4VP corona, which we use as templates for the formation of inorganic ferroelectric nanorods.²⁴ Annealing for longer periods than the 20 h originally used results in even better alignments.

Finally, we have also annealed an asymmetric system with a relatively large PS block. Annealing P141(PDP) $_{1.0}$ under the same conditions as the other samples resulted in terraces with a lamellar morphology, again comparable to the morphology of P3546(PDP) $_{0.1}$, with P4VP(PDP) wetting both the SiO $_2$ and the air interface. However, even though the PDP:4VP ratio is now 1:1, which should be an optimal value for the ODT of P4VP(PDP), terraces within terraces have not at all been observed. This means, that the ability to form terraces within

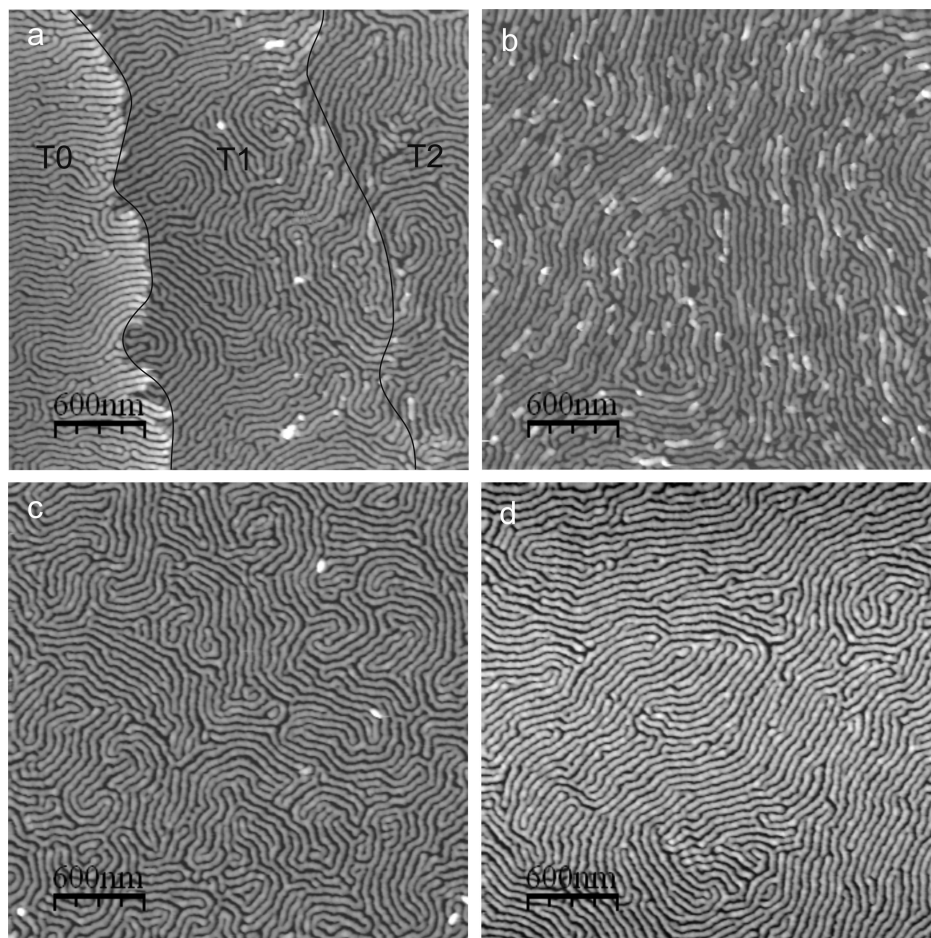


Figure 8. Height AFM images of P110(PDP)_{1.5} annealed for 20 h and subsequently treated with ultrasound in ethanol. Key: (a) $T_s = 20\text{ }^{\circ}\text{C}$, $\Delta z = 55\text{ nm}$, (b) $T_s = 21\text{ }^{\circ}\text{C}$, $\Delta z = 65\text{ nm}$, (c) $T_s = 19\text{ }^{\circ}\text{C}$, $\Delta z = 45\text{ nm}$, and (d) first 20 h at $T_s = 21\text{ }^{\circ}\text{C}$ and then 20 h at $T_s = 19\text{ }^{\circ}\text{C}$, $\Delta z = 30\text{ nm}$.

terraces decreased with a decreasing P4VP(PDP)_{1.0} fraction for the used comb-copolymer systems (P3546(PDP)_{1.0} > P110(PDP)_{1.0} > P141(PDP)_{1.0}), which is logical because a large PS fraction hinders the movement of the now much smaller P4VP(PDP) combs to an orientation which is parallel to the large length scale, as the preferred orientation is perpendicular. This also explains why up to now this phenomenon was not observed, as our previous study only focused on systems with a relatively large PS block.

Conclusion

We have studied the thin film behavior of asymmetric PS-*b*-P4VP(PDP) comb-shaped supramolecules with relatively high comb fractions. In bulk, these systems are known to microphase separate into structures *within* structures, where the large length scale is oriented perpendicular to the short length scale. In thin films, these systems were shown to form terraces of parallelly oriented PS microdomains in a matrix of disordered P4VP(PDP) during annealing in chloroform vapor. Upon evaporation of the solvent, P4VP(PDP) dropped below its ODT, and due to preferential interactions of P4VP with SiO₂ and of PDP with the air interface, formed lamellar layers of the short P4VP(PDP) length scale which were oriented parallel to these interfaces and therefore also to the large length scale structure. This effect was less pronounced for lower ratios of PDP:P4VP due to the lower ODT of the P4VP(PDP) comb in such systems. The effect was also less pronounced for systems with a longer PS block, where it is less easy for the relative short P4VP chains to form loops and move in an orientation which is different from the equilibrium perpendicular orientation.

The mobility of the block copolymers was found to depend on the fraction of PDP. Addition of PDP substantially improves the mobility, however, smaller amounts of PDP showed to be more effective than larger fractions. Although the reason for this is not clear, this behavior has to be a result of concentration dependent solubility of the small molecules in the complicated four component (PS, P4VP, PDP, and CHCl₃) systems.

By washing away PDP from a parallelly oriented cylindrical thin film through ultrasound treatment in ethanol, a monolayer of ordered cylinders with uniform thickness could be obtained, which can serve as a template for the production of inorganic nanorods.

References and Notes

- (1) Lazzari, M.; López-Quintela, M. A. *Adv. Mater.* **2003**, *15*, 1583–1594.
- (2) Cheng, J. Y.; Ross, C. A.; Smith, H. I.; Thomas, E. L. *Adv. Mater.* **2006**, *18*, 2505–2521.
- (3) Olsen, B. D.; Segalman, R. A. *Macromolecules* **2006**, *39*, 7078–7083.
- (4) Matsushita, Y. *Macromolecules* **2007**, *40*, 771–776.
- (5) Hammond, M. R.; Mezzenga, R. *Soft Matter* **2008**, *4*, 952–961.
- (6) Hamley, I. W. *The Physics of Block Copolymers*; Oxford Science Publications: Oxford, U.K., 1998.
- (7) Darling, S. B. *Prog. Polym. Sci.* **2007**, *32*, 1152–1204.
- (8) Horvat, A.; Lyakhova, K. S.; Sevink, G. J. A.; Zvelindovsky, A. V.; Magerle, R. *J. Chem. Phys.* **2004**, *120*, 1117–1126.
- (9) Lyakhova, K. S.; Sevink, G. J. A.; Zvelindovsky, A. V.; Horvat, A.; Magerle, R. *J. Chem. Phys.* **2004**, *120*, 1127–1137.
- (10) Fasolka, M. J.; Mayes, A. M. *Annu. Rev. Mater. Res.* **2001**, *31*, 323–355.
- (11) Krausch, G.; Magerle, R. *Adv. Mater.* **2002**, *14*, 1579–1583.
- (12) Segalman, R. A. *Mater. Sci. Eng. Res.* **2005**, *48*, 191–226.
- (13) van Zoelen, W.; Asumaa, T.; Ruokolainen, J.; Ikkala, O.; ten Brinke, G. *Macromolecules* **2008**, *41*, 3199–3208.

- (14) Tokarev, I.; Krenek, R.; Burkov, Y.; Schmeisser, D.; Sidorenko, A.; Minko, S.; Stamm, M. *Macromolecules* **2005**, *38*, 507–516.
- (15) Zhang, P.; Gao, J.; Li, B.; Han, Y. *Macromol. Rapid Commun.* **2006**, *27*, 295–301.
- (16) Albrecht, K.; Mourran, A.; Zhu, X.; Markkula, T.; Groll, J.; Beginn, U.; de Jeu, W. H.; Moeller, M. *Macromolecules* **2008**, *41*, 1728–1738.
- (17) Ruokolainen, J.; Mäkinen, R.; Torkkeli, M.; Mäkelä, T.; Serimaa, R.; Ikkala, O.; ten Brinke, G. *Science* **1998**, *280*, 557–560.
- (18) Tung, S.-H.; Kalarickal, N. C.; Mays, J. W.; Xu, T. *Macromolecules* **2008**, *41*, 6453–6462.
- (19) Elbs, H.; Krausch, G. *Polymer* **2004**, *45*, 7935–7942.
- (20) Lee, S. H.; Kang, H.; Kim, Y. S.; Char, K. *Macromolecules* **2003**, *36*, 4907–15.
- (21) Ruokolainen, J.; Torkkeli, M.; Serimaa, R.; Komanshek, B. E.; Ikkala, O.; ten Brinke, G. *Phys. Rev. E* **1996**, *54*, 6646–6649.
- (22) Valkama, S.; Ruotsalainen, T.; Nykänen, A.; Laiho, A.; Kosonen, H.; ten Brinke, G.; Ikkala, O.; Ruokolainen, J. *Macromolecules* **2006**, *39*, 9327–9336.
- (23) Horvat, A.; Sevink, A.; Zvelindovsky, A. V.; Krekhov, A.; Tsarkova, L. *ACS Nano* **2008**, *2*, 1143–1152.
- (24) To be published.

MA801814W